Circulation: Genomic and Precision Medicine

ORIGINAL ARTICLE

Estimating the Posttest Probability of Long QT Syndrome Diagnosis for Rare *KCNH2* Variants

Krystian Kozek, PhD, MD; Yuko Wada, PhD, MD; Luca Sala, PhD; Isabelle Denjoy, MD, PhD; Christian Egly, PharmD; Matthew J. O'Neill, BS; Takeshi Aiba, PhD, MD; Wataru Shimizu, PhD, MD; Naomasa Makita, PhD, MD; Taisuke Ishikawa, DVM, PhD; Lia Crotti, MD, PhD; Carla Spazzolini, DVM, MS; Maria-Christina Kotta, MSc, PhD; Federica Dagradi, MD; Silvia Castelletti, MD; Matteo Pedrazzini, MSc; Massimiliano Gnecchi, MD, PhD; Antoine Leenhardt, MD; Joe-Elie Salem, MD, PhD; Seiko Ohno, MD, PhD; Yi Zuo, MPH; Andrew M. Glazer, PhD; Jonathan D. Mosley, MD, PhD; Dan M. Roden, MD; Bjorn C. Knollmann, MD, PhD; Jeffrey D. Blume, PhD; Fabrice Extramiana, MD, PhD; Peter J. Schwartz, MD; Minoru Horie, MD, PhD; Brett M. Kroncke, PhD

BACKGROUND: The proliferation of genetic profiling has revealed many associations between genetic variations and disease. However, large-scale phenotyping efforts in largely healthy populations, coupled with DNA sequencing, suggest variants currently annotated as pathogenic are more common in healthy populations than previously thought. In addition, novel and rare variants are frequently observed in genes associated with disease both in healthy individuals and those under suspicion of disease. This raises the question of whether these variants can be useful predictors of disease. To answer this question, we assessed the degree to which the presence of a variant in the cardiac potassium channel gene *KCNH2* was diagnostically predictive for the autosomal dominant long QT syndrome.

METHODS: We estimated the probability of a long QT diagnosis given the presence of each *KCNH2* variant using Bayesian methods that incorporated variant features such as changes in variant function, protein structure, and in silico predictions. We call this estimate the posttest probability of disease. Our method was applied to over 4000 individuals heterozygous for 871 missense or in-frame insertion/deletion variants in *KCNH2* and validated against a separate international cohort of 933 individuals heterozygous for 266 missense or in-frame insertion/deletion variants.

RESULTS: Our method was well-calibrated for the observed fraction of heterozygotes diagnosed with long QT syndrome. Heuristically, we found that the innate diagnostic information one learns about a variant from 3-dimensional variant location, in vitro functional data, and in silico predictors is equivalent to the diagnostic information one learns about that same variant by clinically phenotyping 10 heterozygotes. Most importantly, these data can be obtained in the absence of any clinical observations.

CONCLUSIONS: We show how variant-specific features can inform a prior probability of disease for rare variants even in the absence of clinically phenotyped heterozygotes.

Key Words: genetic variation ■ heterozygotes ■ ion channel ■ long QT syndrome ■ phenotype

Sequencing an individual's full genome or exome now costs less than many routine medical procedures. One resulting vision is that our genomes could be sequenced early in life for individualized medical advice about disease prevention and drug selection. However, most discovered variants will never be observed in a sufficient number of heterozygotes for a definitive association with disease.[1,2] Furthermore, even when a variant is strongly associated with disease, the clinical implications can vary strikingly across individuals.[3,4]

The American College of Medical Genetics and Genomics put forward an interpretation framework that integrates

Correspondence, Brett Kroncke, PhD, Department of Medicine, Vanderbilt University Medical Center, 2215B Garland Ave, 1215E MRBIV, Nashville, TN 37232. Email brett.m.kroncke.1@vumc.org

The Data Supplement is available at https://www.ahajournals.org/doi/suppl/10.1161/CIRCGEN.120.003289.
For Sources of Funding and Disclosures, see page 504.

Circulation: Genomic and Precision Medicine is available at www.ahajournals.org/journal/circgen

Nonstandard Abbreviations and Acronyms

AUC	area under a receiver operating characteristic curve
LQT2	long QT syndrome type 2
WT	wild-type

criteria, such as variant prevalence, function, and computational predictions, into a single annotation from benign to pathogenic.[5,6] Each additional satisfied criterion raises or lowers the probability the variant is classified pathogenic.[6] However, even definitively annotated pathogenic variants have heterogeneous or asymptomatic clinical presentations,[7,8] and variants annotated benign may still increase risk (see Discussion). Thus, the predictive value of rare variants remains unclear.[9,10] Because a positive test for most variants cannot be applied to enough heterozygous individuals to achieve a definitive association with disease, a statistical approach is required to estimate the posttest probability of disease and validate those predictions in different groups and cohorts.

The observation of a single (or few) heterozygous carrier(s) does not adequately inform the probability of disease. Rather, individuals heterozygous for these variants benefit from a prior probability informed by knowledge about their clinical characteristics or the population they are drawn from. This prior, informed without knowledge of the variant, more reasonably reflects the true disease probability. In contrast, we propose to construct a prior probability of disease conditioned on variant-specific features and to modify this estimate using observations of heterozygous carriers. Our analysis yields a prior probability conditioned on variant-specific features known to be relevant to the association between the gene and disease. In practice, disease probability estimates are calibrated largely by how variant features associate with disease probability in well-characterized variants. Our final estimate is effectively the posttest probability of disease given the presence of a variant or the positive predictive value of rare genetic variants. We use posttest probability interchangeably with penetrance, in which the former recapitulates diagnostic thinking and reflects the Bayesian framework of this approach.

In past work, we described an algorithm for estimating the probability of a diagnosis of Brugada syndrome given the presence of a variant in the cardiac sodium channel gene *SCN5A*.[11] Although we incorporated variant-specific covariates (eg, sequence conservation, functional perturbation, structural location, etc), Brugada syndrome is likely oligogenic and the clinical phenotype is sometimes difficult to assess. In this article, we develop a similar algorithm for estimating the probability of long QT syndrome type 2 (LQT2), a well-characterized and monogenic disorder induced by variants in the cardiac potassium channel gene *KCNH2* (also called the human Ether-a-go-go-Related Gene, or *hERG*).

The *KCNH2* gene encodes an ion channel subunit that assembles into the homotetrameric $K_V11.1$ potassium channel. This channel produces the rapid delayed-rectifier repolarizing current, I_{Kr}, which sustains cardiomyocyte repolarization throughout the action potential plateau phase.[12,13] Loss-of-function *KCNH2* variants that reduce I_{Kr} are associated with LQT2, a congenital heart arrhythmia defined by a prolongation of the QT interval on an ECG. Individuals with this ECG feature are at a greater risk for torsades de pointes, a life-threatening arrhythmia. With our method, we estimate the probability that an individual heterozygous for a missense or in-frame insertion/deletion variant in *KCNH2* presents with LQT2 (for each variant). We validated our approach in an international cohort of 933 individuals ascertained under suspicion of LQTS, heterozygous for 266 unique missense, and in-frame insertion/deletion variants in *KCNH2*. Our results suggest the probability of disease can be estimated accurately before knowing the phenotype of a given heterozygous individual. Our result is a point estimate and 95% credible interval of disease probability for each variant which can be calculated before observing a single heterozygote. This prior—conditioned on variant-specific features—can be directly combined with observed heterozygotes for a posterior probability of disease. In this way, the prior is comparable with observations of heterozygotes, we estimate roughly 10 observations. All data resulting from this study are presented in web-accessible format at https://variantbrowser.org/KCNH2/ (Figure I in the Data Supplement).

METHODS

All data and materials are publicly available on GitHub (https://github.com/kroncke-lab/Bayes_KCNH2_LQT2_Penetrance). Additionally, a compiled and curated form of the data presented here are available in the *KCNH2* Variant Browser (https://variantbrowser.org/KCNH2/; Figure I in the Data Supplement). Internal Review Board (no. 191563) was evaluated at Vanderbilt University Medical Center and found to meet 45 CFR 46.104 (d) category (4) for Exempt Review. Detailed methods are available as Data Supplement.

RESULTS

KCNH2 Variant Heterozygote Datasets

In total, the literature combined with the Genome Aggregation Database (gnomAD) produced 871 unique missense or insertion/deletion (in-frame insertion/deletion) *KCNH2* variants; 4810 individuals were heterozygous for these variants (<0.001 minor allele frequency), 1041 of which were diagnosed with LQT2 according to our classification criteria (see Materials and Methods for details). From 5 arrhythmia centers in France, Italy, and Japan, we collected a cohort of patients heterozygous for *KCNH2*

variants. From these sites, we identified 266 unique missense or in-frame insertion/deletion variants in *KCNH2*, 933 heterozygote carriers of these variants, 594 of which met our criteria for LQT2. From this cohort, the average age of diagnosis or ascertainment (if criteria for affected status were not met) within the participating sites was 24 years old (SD of 19 years; available for 744 individuals in the cohort dataset). Gender was distributed (744 individuals in the cohort dataset); 45% were male.

Rates of LQT2, Observed in the Literature and Our Cohort, Is Associated With In Vitro and In Silico Features

To assess the association between in vitro and in silico characteristics of $I_{Kr}/K_V11.1$/*KCNH2* and the fraction of heterozygotes which present with LQT2, we calculated nonparametric Spearman rank-order coefficients (Spearman ρ) between these features and the observed literature (Figure 1, black) or cohort (Figure 1, red) LQT2 probability (the fraction of heterozygotes diagnosed with LQT2 over total number of heterozygotes). We evaluated common in silico predictors, electrophysiological parameters for I_{Kr}, and a by-residue average observed LQT2 probability in a 3-dimensional shell surrounding each residue (LQT2 probability density, see Materials and Methods for details). The variant-specific features LQT2 probability density, rare exome variant ensemble learner (REVEL), and heterologous measurement of variant I_{Kr} peak tail currents had Spearman ρ absolute value point estimates around 0.6 and 0.7 in the literature and cohort datasets, the highest that reached a nominal *P* value of 0.05.

Two broad in silico variant classifiers, Protein Variation Effect Analyzer (PROVEAN) and Polymorphism Phenotyping v2 (PolyPhen-2), had lower Spearman ρ point estimates than structure and peak tail currents (weighted Spearman ρ of 0.39 and −0.59 in the literature dataset and 0.33 and −0.46 in the cohort set for PolyPhen-2 and PROVEAN, respectively), although still statistically significant. Repeating this analysis in the cohort dataset produced mostly lower coefficients, although many retained statistical significance (Figure 1). Several biophysical properties were not statistically significant in either dataset.

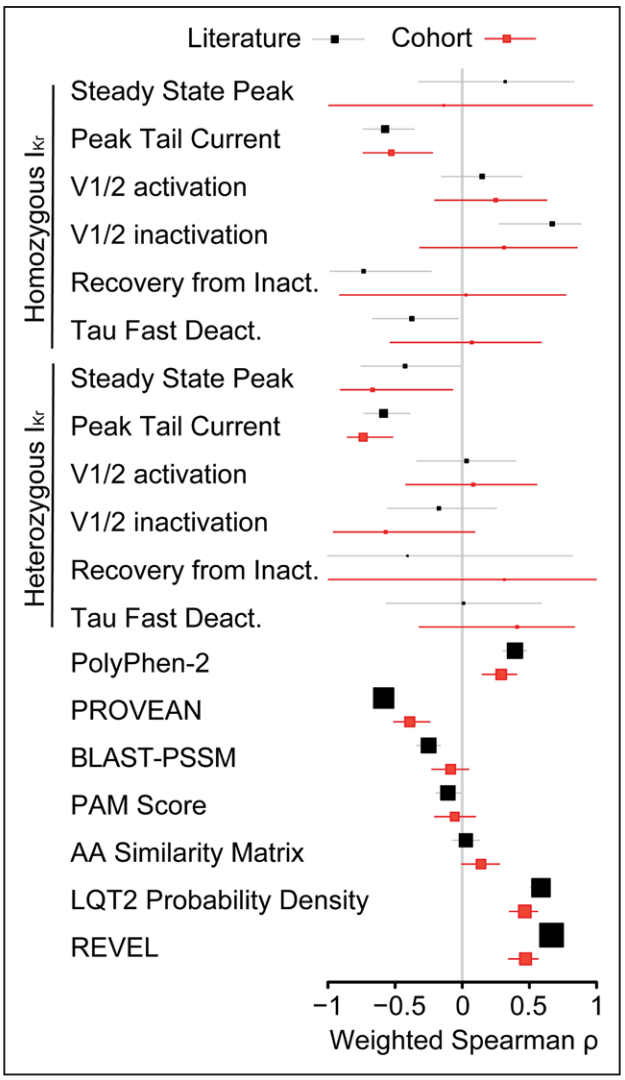

Figure 1. Weighted Spearman correlations between the fraction of heterozygotes diagnosed with long QT syndrome type 2 (LQT2) in the literature or cohort and the listed features for each variant.
Weighted Spearman correlations between the fraction of heterozygotes diagnosed with LQT2 in the literature and listed features for each variant. Black and red squares indicate the estimate for the weighted Spearman correlation, weighted by 1−1/(0.01+total heterozygotes), for the literature and cohort dataset, respectively. The gray and red lines indicate 95% CIs (obtained by bootstrap), respectively. Larger box sizes indicate greater number of variants included in calculation. BLAST-PSSM indicates basic local alignment search tool position-specific scoring matrix; PAM score, point accepted mutation score; PROVEAN, protein variation effect analyzer; and REVEL, rare exome variant ensemble learner.

Magnitude of LQT2 Probability Varies By Residue Location in 3-Dimensional Space

Given the relatively high correlation between LQT2 probability density and observed LQT2 probability, we mapped LQT2 probability density onto the structure of $K_V11.1$ (Figure 2, Figures II and III in the Data Supplement). Figure 2 and Figure II in the Data Supplement demonstrate LQT2 penetrance is not uniformly distributed over the major domains in $K_V11.1$ (see Figure II in the Data Supplement for specific examples). This is in contrast to averaging over variants in sequence space as shown in Figure IV in the Data Supplement and done previously.[14,15] For instance, the transmembrane segment in $K_V11.1$ includes the voltage-sensing domains and pore domains, each of which has their own subdomains with high or low LQT2 penetrance. Some of these subregions are very small, localized to only a few contacting residues. For example, the voltage-sensing domain has a relatively low penetrance

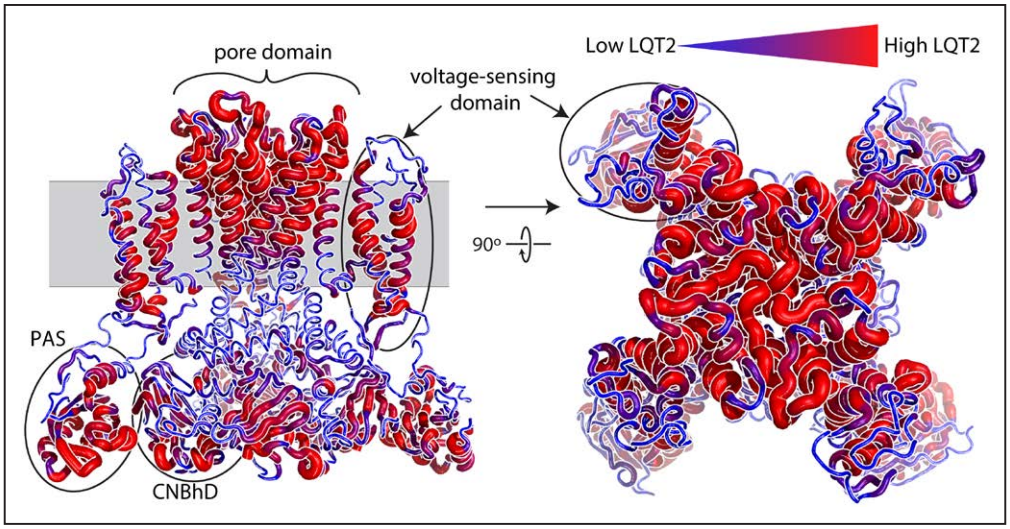

Figure 2. Long QT syndrome type 2 (LQT2) probability density mapped on to K_V11.1 structure.
LQT2 probability density mapped on to the three-dimensional structure of the K_V11.1 channel. Larger and redder segments indicate higher LQT2 probability density; smaller and bluer segments indicate lower LQT2 probability density. The model illustrates structural information regarding amino acids predicted to increase disease probability. Unlike linear graphical displays identifying pathogenic loci, LQT2 probability density provides novel, three-dimensional, insights into the specific structural components of the Per-Arnt-Sim (PAS), C-terminal cyclic nucleotide-binding homology domain (CNBhD), voltage-sensing, and pore domains that are associated with increased prevalence of LQT2.

density in the intracellular half of helices S2 and S3 (Figure II in the Data Supplement), whereas the most highly penetrant residues in this domain are in helices S1 and S4, which contact the pore domain near the midpoint of the membrane bilayer. Similarly, the pore domain shows the highest penetrance density near the selectivity filter and decreases towards the intracellular face of the pore. Additionally, the N-terminal Per-Arnt-Sim domain and C-terminal cyclic nucleotide-binding homology domain, both having relatively high observed LQT2 penetrance overall (Figure II in the Data Supplement), are also heterogeneous. The most highly penetrant residues in these domains exist near the contacting surfaces between and among these domains. These trends are more muted in the in the observed LQT2 probability from cohort and literature data viewed linearly (Figure IV in the Data Supplement).

Estimated Posttest Probability of LQTS Based on *KCNH2* Variants Found in Only One Heterozygote Is Predictive

Variants found in only a single known heterozygous individual are the largest class of variants in the literature and our cohort data. Accordingly, we split the data into 2 groups: (1) variants with ≥2 heterozygous individuals and (2) variants with only one heterozygous individual (Figure V in the Data Supplement). We then estimated the posttest probabilities of LQTS based on *KCNH2* variants from group 1 (those with at least two heterozygous individuals). A Bayesian model was fit using an expectation-maximization algorithm (see Materials and Methods for details and Kroncke et al[11]). The predictive ability of our posttest LQT2 probability estimates was evaluated using the area under a receiver operating characteristic curve (AUC) from group 2, those found in only one heterozygous individual (Figure 3 and Figure V in the Data Supplement). Additionally, we evaluated models fit on the full literature dataset on variants found in the cohort dataset (Figure 3, bottom, and Figures V and VI in the Data Supplement). In all cases, the estimated AUC from our method outperformed other existing algorithms (LQT2 probability density, REVEL, PROVEAN, PolyPhen-2, BLAST-PSSM [basic local alignment search tool position-specific scoring matrix], and PAM score [point accepted mutation score]). For single heterozygotes in the literature, we observed AUCs of 0.87, 0.84, and 0.83 for our posttest probability model, REVEL, and LQT2 probability density, respectively. PROVEAN and PolyPhen-2, with AUCs of 0.74 and 0.73, respectively, were lower than our method and REVEL, as expected, since REVEL included PROVEAN and PolyPhen-2 as predictive covariates during construction.[16] For variants with single heterozygotes in the cohort dataset (Figure 3, bottom), AUC point estimates were lower overall, 0.78 and 0.77 for our method and LQT2 probability density, respectively. Surprisingly, REVEL scores were much less predictive in this group of variants, producing an AUC of 0.65, compared with 0.84 in the literature dataset. These differences in AUCs were also present when all variants were included and evaluated at various observed probability cutoffs (Figure VI in the Data Supplement). Previously published in silico predictors PROVEAN and PolyPhen-2 each had an AUC of 0.70, similar for the literature and cohort.

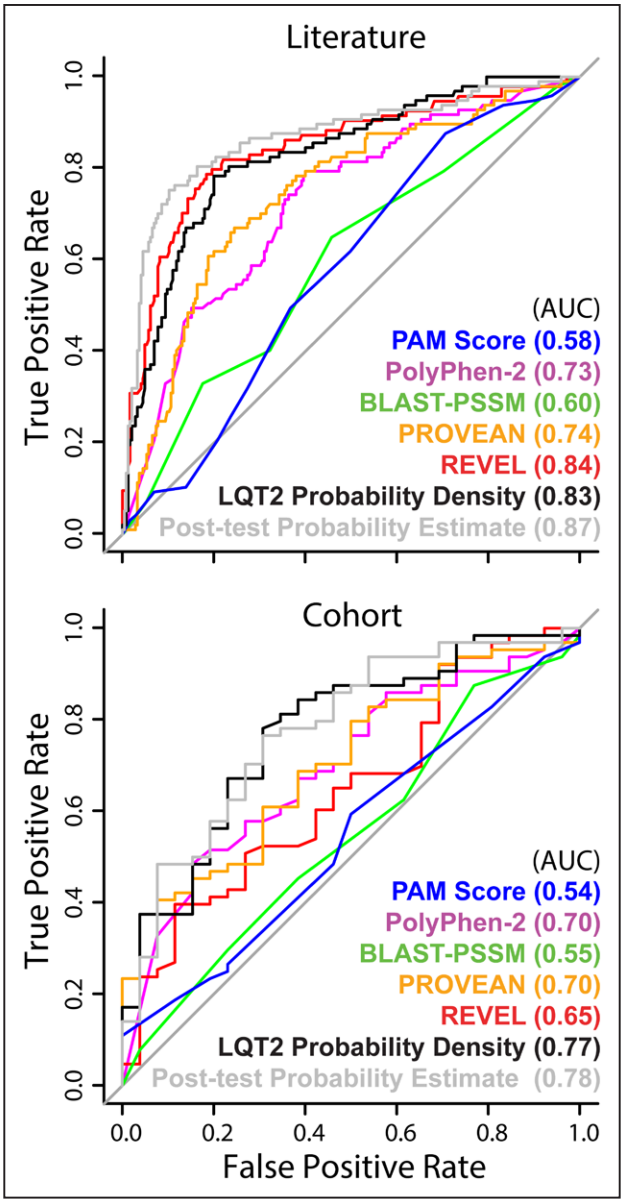

Figure 3. Receiver operating characteristic curves of features sorting variants with only one heterozygote observed.
Receiver operating characteristic curves from predictors against variants with only one observation, an individual affected with long QT syndrome type 2 (LQT2) or not, in the cohort (Figure V in the Data Supplement). The carriers come from either the literature (above) or the cohort (below). The estimated posttest probability and LQT2 probability density were not exposed to the evaluation variants, those whose heterozygote count is equal to one, during training. All cohort data were withheld from the expectation maximization calculation and LQT2 probability density during construction (Figure V in the Data Supplement). AUC indicates area under the curve; BLAST-PSSM, basic local alignment search tool position-specific scoring matrix; PROVEAN, protean variation effect analyzer; REVEL, rare exome variant ensemble learner.

Posttest LQT2 Probability Estimates Are Improved By Including *KCNH2* Variant Features

The R^2 between our LQT2 probability estimates and the cohort observed LQT2 probability is 0.30 when all variants are included, higher than in silico classifiers or LQT2 probability density; R^2 estimates are higher overall when restricting to the set of variants where heterozygously collected peak tail current is known (Table and Table I in the Data Supplement).

Table. Weighted R^2 Between the Fraction of Heterozygotes Diagnosed With LQT2 in the Literature and Cohort With Estimates

LQT2 probability estimates	Literature (n=706)*	Cohort (n=246)*
LQT2 probability density	0.49 [0.39–0.60]	0.23 [0.12–0.34]
REVEL	0.38 [0.31–0.44]	0.21 [0.11–0.33]
Posttest LQT2 probability	0.82 [0.77–0.86]	0.30 [0.19–0.43]

LQT2 indicates long QT syndrome type 2; and REVEL, rare exome variant ensemble learner.
*Weighted R^2 [95% CI] for the same subset of variants, weighted by 1-1/(0.01+total heterozygotes), n is the number of unique *KCNH2* variants.

Because probability estimates are generally more reliable as the number of phenotyped heterozygous individuals increases, we calculated R^2 at varying cutoffs of heterozygote count (Figure 4). As we restrict the analysis to variants with higher numbers of heterozygotes, we see R^2 between our LQT2 posttest probability predictions and observed LQT2 probability substantially increase in both datasets (Figure 4). This shows that LQT2 probability predictions are statistically significant across sources.

gnomAD Data Are Critical to Build the Most Robust LQT2 Probability Estimates

When gnomAD heterozygotes are removed from the literature dataset, the mean weighted probability observed in the cohort and the literature sets are closer to each other; this is also reflected in empirical probability distributions (Figure VII in the Data Supplement). However, rank-order correlation between the literature and the cohort was reduced: without gnomAD, Spearman ρ between literature and cohort was 0.26 (95% CI, 0.01–0.50); when gnomAD was added to the literature, ρ=0.35 (95% CI, 0.11–0.58); and when gnomAD was added to the cohort, ρ=0.33 (95% CI, 0.09–0.55). In addition, predictive models trained from the literature without gnomAD resulted in lower AUCs and R^2s, due in part to the reduced information in the LQT2 probability density feature (Table II in the Data Supplement and Figures VIII and IX in the Data Supplement). These results demonstrate the importance of including control variants, such as those from gnomAD, in the LQT2 posttest probability estimates.

Example LQT2 Probability Estimates for a Segment of K_V11.1

The outcome of our analysis is a range of data-driven posttest probabilities for each variant, initial probabilities conditioned on variant-specific properties, and posterior probabilities after heterozygous individuals are added. Each estimate is a probability distribution with a 95%

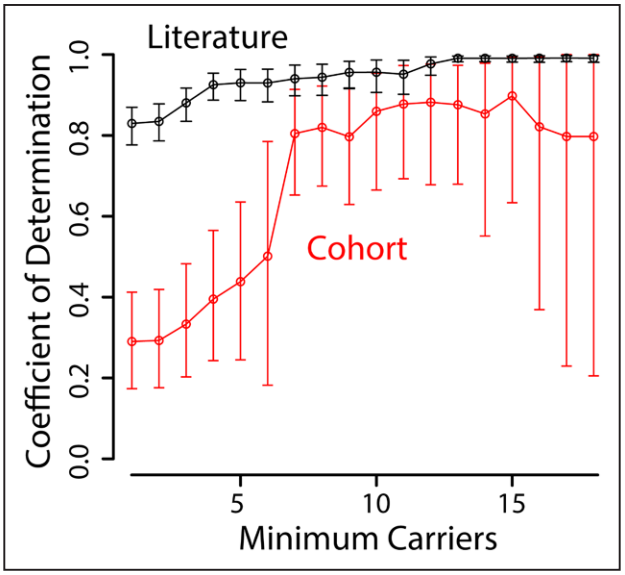

Figure 4. Coefficient of determination determined for long QT syndrome type 2 (LQT2) posttest probability predictions and fraction of homozygotes diagnosed with LQT2 from the cohort or literature.
Coefficient of determination determined between expectation maximization LQT2 probability predictions and observed LQT2 probability from the cohort or literature. There are fewer variants to analyze as we restrict to variants with higher heterozygote counts.

credible interval. We illustrate the outcome of this method for variants in a segment within $K_V11.1$ from p.Leu622 (c.1866) to p.Arg752 (c.2255) in Figure 5. Residues towards the extracellular face of $K_V11.1$ have a higher prior and posterior estimated probability. The LQT2 probability prior probabilities conditioned on heterozygously collected peak tail current, LQT2 probability density, and REVEL score, are near the observed probability (LQT2/total heterozygotes) for most variants (Figure 5).

Equivalence Between *KCNH2* Variant Features and Clinically Phenotyped Heterozygotes

The width of initial prior probability intervals conditioned on variant features (Figure 5, solid-colored lines) are determined by choice of ν in Equation 1 as previously described[11]:

$$\sigma_i = \frac{\mu_i(1-\mu_i)}{1+\nu} \quad (1)$$

where ν represents the number of observations in the beta-binomial model, in this case, clinically phenotyped individuals heterozygous for variants in *KCNH2,* σ_i is the variance in the beta-binomial model and. μ_i is the mean penetrance estimate for the i^{th} variant. As ν grows, the prior 95% interval narrows; as ν decreases, prior 95% intervals expand. For very large ν, for example, ν=100, the posterior estimates of LQT2 posttest probability are heavily influenced by the prior such that very many observations of heterozygotes (1000–10 000) are required to significantly change the posterior. At the other extreme of very small ν, for example, ν=1, the posterior estimates of LQT2 probability are largely independent of the priors. Acceptable values of ν would be those where 95% of variants have true LQT2 probabilities within the posterior 95% credible interval. To find values of ν where this was the case, we calculated posterior coverage rates by adding hypothetical heterozygotes sampled at the observed LQT2 probability to the prior generated with multiple values of ν, as described in the Data Supplement and shown in Figures X through XII in the Data Supplement. This procedure resulted in a range of acceptable ν values near ν=10. Heuristically, for each variant, the posttest estimate of LQT2 probability carries the information equivalent to clinically phenotyping ≈10 heterozygotes.

DISCUSSION

Spectrum and Example of LQT2 Diagnosis Probability Attributable to *KCNH2* Variants

Few *KCNH2* coding variants have been discovered in a sufficiently large population to reliably estimate their posttest probability of developing LQT2 as defined in the Materials and Methods. However, variants such as p.Lys897Thr (c.2690A>C), p.Arg176Trp (c.526C>T), p.Val822Met (c.2464G>A), and p.Ala561Val (c.1682C>T) have been observed in many clinically phenotyped individuals both in the literature and in our assembled cohort. These variants span both the spectrum of channel defect (measured as heterozygously collected peak tail current compared to wild-type [WT]) and spectrum of LQT2 disease probability. The most common *KCNH2* coding variant, p.Lys897Thr, induces a very modest channel phenotype (peak tail current 78% of WT)[17] and is common enough (5%–24% of alleles)[18] to preclude a large influence in LQT2 diagnosis, though its presence may modify risk.[17] p.Arg176Trp induces peak tail current between 50% and 75% of WT[19,20] and has a well-established LQT2 probability, estimated at 20%.[21] We observe a similar LQT2 probability of 35% in the literature and 43% in the cohort, with higher values likely reflecting a bias in ascertainment (also discussed below). p.Val822Met induces a significant channel defect, peak tail current of 44% of WT,[22] and we correspondingly observe a higher LQT2 probability from the literature (65%)[23,24] and cohort (60%). p.Ala561Val induces a severe channel defect, peak tail current between 0 and 46% of WT with a mean near 20%[25–28]; we observed an LQT2 probability of 91% from the literature and 88% from the cohort. These variants illustrate that molecular defects induced by genetic variants in *KCNH2* place heterozygotes at higher risk for LQT2.

Our framework allows us to exploit this relationship in part by conditioning estimates of disease probability on these defects, directly (in vitro data) or indirectly (in silico

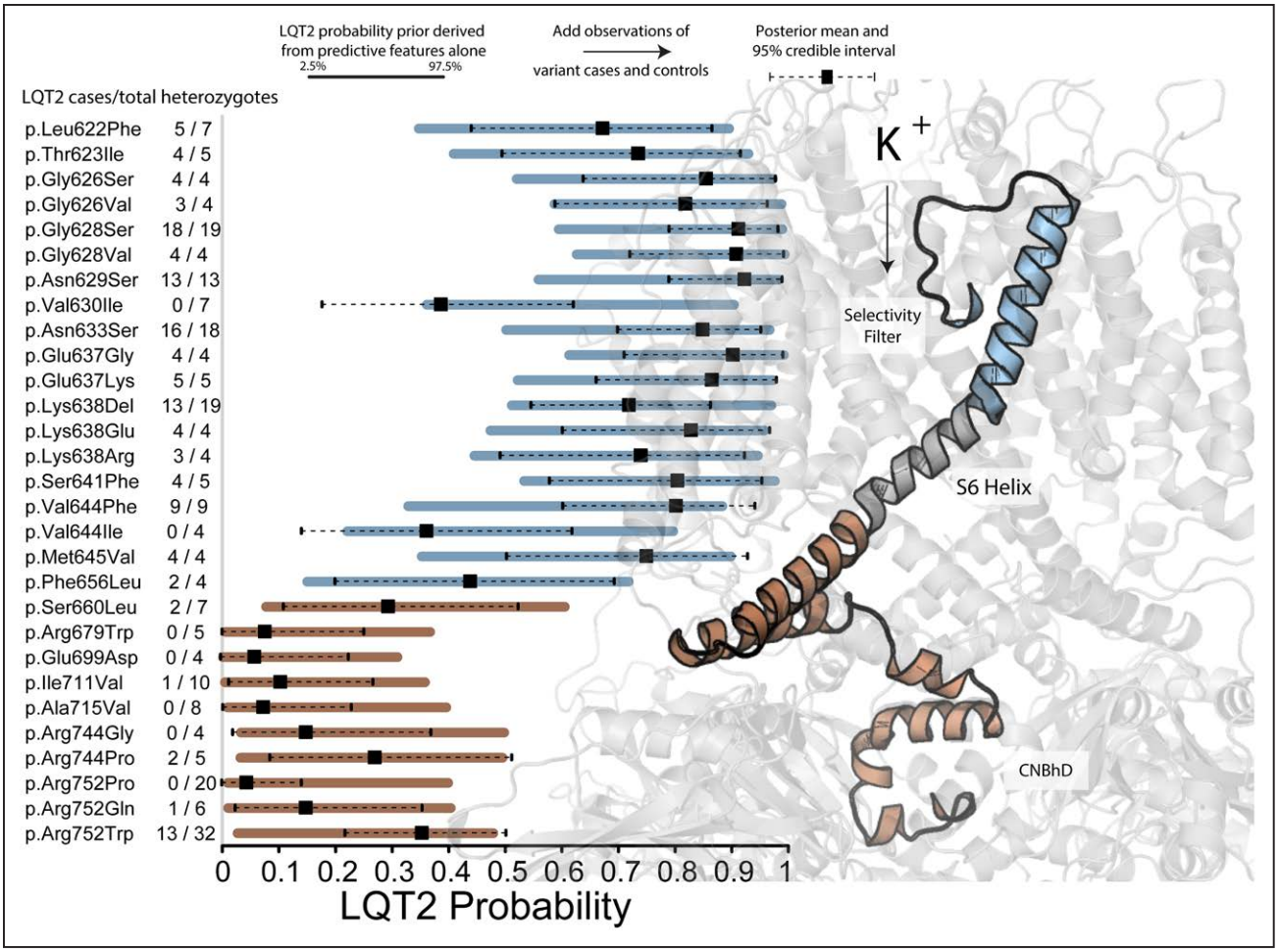

Figure 5. Example probability predictions for segment of *KCNH2* including the selectivity filter and S6 helix.
Example probability predictions for segment of *KCNH2* including the selectivity filter and S6 helix. Priors were generated from in vitro (when available) and in silico covariates. Bars indicate the 95% interval of the prior. The dot and lines reflect the point estimate and 95% credible interval of the posterior, after the observations of affected individuals, and those not meeting the threshold for affected status are included. Number of heterozygotes follows variant name on the **left** side of the figure. To the **right** is a translucent structure of the K_V11.1 channel. K_V11.1 from p.Ser621 (c.1863) to p.Arg752 (c.2255) is represented as a solid cartoon, with 2 segments highlighted in different colors. The blue region highlights a segment with higher overall long QT syndrome type 2 (LQT2) probability while the red region highlights a segment with lower overall LQT2 probability. CNBhD indicates C-terminal cyclic nucleotide-binding homology domain.

data). Our resulting model is informed largely by variants with many classified heterozygotes, like the variants just mentioned, but is most useful for variants with few or no known heterozygous carriers. Here, we validated our method with a diverse, international cohort of clinically phenotyped *KCNH2* variant heterozygotes curated from among five centers; the cohort was withheld during all training stages and all potential overlapping individuals were removed. We tested how well our prior LQT2 probability estimates discriminate variants observed once in individuals who do or do not meet the criteria for LQT2 diagnosis (Figure 3) and correlate with the observed LQTS probability/penetrance (Figure 4). Lastly, all performance statistics reported for the probability density covariate were generated using leave-one-out cross-validation, that is, the probability density derived for each variant was never exposed to the observed LQT2 probability/penetrance for that variant.

Structure Combined With Previously Described Variants Produced the Most Predictive Feature of Observed Cohort LQT2 Probability

Variant position in K_V11.1 domains, such as transmembrane, pore, or intracellular, is associated with differential risk of events.[14,29,30] Expanding on this observation, and leveraging the recently determined K_V11.1 channel structure (PDBID: 5VA1),[31] we developed a metric to quantitate average LQT2 probability in the three-dimensional space surrounding each residue (Figure 2 and Figure II in the Data Supplement). The resulting metric, LQT2 probability density, was comparable to the in silico predictor REVEL in terms of AUC and R^2 (Figure 3 and Table). Alone, LQT2 probability density could explain 50% of the variance in LQT2 probability as observed in the literature (Table); this reduced to 23% in the cohort but was still more predictive than even

in vitro heterozygously collected peak tail current data (Table I in the Data Supplement). We attribute at least part of this decrease to greater ascertainment bias and lower heterozygous carrier counts in the cohort dataset. In addition, the R^2 of 0.23 (up to 0.3 when including all covariates) is the most pessimistic coefficient of determination. When restricting to variants with greater heterozygote counts, the R^2 improves to around 0.8 and so we estimate the generalized R^2 is likely closer to a clinically meaningful value.

Bias in Data Collected From the Literature, gnomAD, and Cohort

The clinical environment taxonomizes *KCNH2* variants disproportionately from patients who present with disorders.[32,33] For example, individuals heterozygous for *KCNH2* p.Arg176Trp (annotated in ClinVar variously as a risk factor, Likely Benign, and Variant of Uncertain Significance) have a mean QTc of 459±40 ms in clinical LQT2 families, those with at least one proband, but a mean QTc of 433±27 ms in a cross-sectional cohort of unselected heterozygotes.[34] Similarly, we found most variants in the cohort have higher LQT2 probabilities than what we observed in the literature (Figure 6 and Figure XIII in the Data Supplement). Some of these variants have statistically significant differences in observed LQT2 probability between the datasets (Figure 6B). Although all datasets have biases, adding heterozygous individuals from gnomAD to the available literature yields LQT2 probability estimates more consistent with the cohort (Table II and Figures VIII and IX in the Data Supplement) and we, therefore, suggest the combined datasets produce the most accurate, although flawed, estimate of variant-specific LQT2 probability.

Evidence That Some Variants Classified as Benign Increase the Probability of LQT2 to Higher Than the General Population Rate

Similar to *KCNH2* p.Arg176Trp, variants such as p.Pro347Ser (c.1039C>T), p.Arg148Trp (c.442C>T), p.Ala913Val (c.2738C>T), and p.Arg328Cys (c.982C>T) were previously associated with LQT2[35–39] but are also more common in the general population than is expected for highly penetrant variants.[18] This trend, observed in several variants which also produce a functional perturbation consistent with LQTS, has prompted some to use the label LQT-lite.[40,41] We also observed these variants in affected individuals in the cohort (2 out of 5, 4 out of 19, 1 out of 4, and 1 out of 2 heterozygotes, respectively). The most recent classifications for these variants in ClinVar are benign or likely benign. However, we estimate the probability of LQTS for heterozygous carriers of these variants at around 2% or higher, much greater than the ≈0.04% in the general population. These data suggest

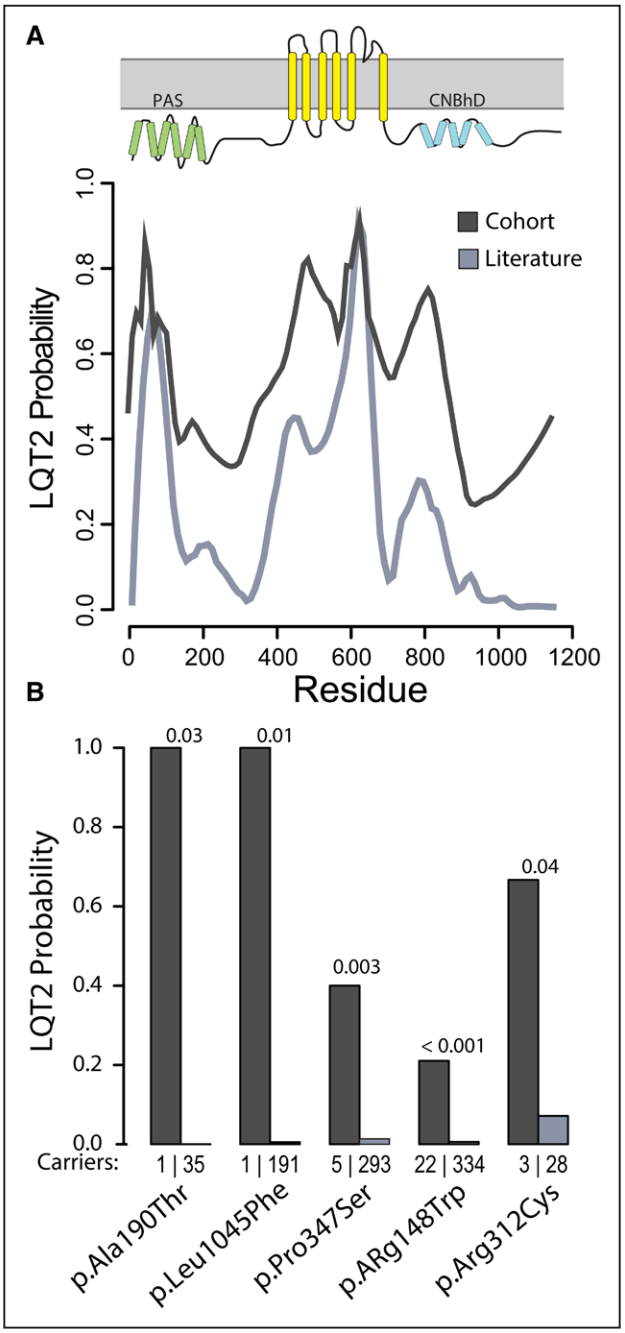

Figure 6. Ascertainment bias in long QT syndrome type 2 (LQT2) probability for *KCNH2* variants from the arrhythmia center cohort compared to the literature.
A, The 30-residue moving average of LQT2 probability for each amino acid over the entire $K_v11.1$ channel for data acquired from the cohort (dark gray) and collected from the literature (light gray; see Figure IV in the Data Supplement for the distribution of variants used in the calculation). Ascertainment bias is evident by the higher overall LQT2 probability in the cohort dataset compared to the literature (which includes the Genome Aggregation Database). **B**, Observed probability (literature and the cohort) for a selected set of *KCNH2* variants, *P* values from the Fisher exact test between the observations of heterozygotes in the literature and in the cohort. The observed probability for many variants from the cohort is significantly higher than that calculated from the literature. The number of heterozygous carriers discovered in each group is shown directly above the variant names. CNBhD indicates C-terminal cyclic nucleotide-binding homology domain; and PAS, Per-Arnt-Sim.

some variants classified as benign or likely benign are truly disease-causing for a small fraction of patients.

Application of Bayesian Probability to Arrhythmia Genetics Clinics

Bayesian reasoning has long been at the core of clinical diagnosis. Given that the majority of heterozygous carriers of *KCNH2* variants found in arrhythmia genetics clinics (or elsewhere) carry ultrarare or novel variants, we anticipate that this prior, trained on variant-specific features will have direct clinical utility to the clinician. The addition of 10 equivalent observations for a previously unreported or seldomly reported variant can directly guide clinical management and establish a threshold of intervention with drug treatment or simple clinical observation. Additionally, this method helps overcome ascertainment bias prevalent in clinically-obtained data since the prior is trained on variant-specific features agnostic to clinical information (Figures 5 and 6). Although there is no intention to replace clinical phenotyping, we do anticipate the ability to augment clinical reasoning through a more accurate prior when combining clinical and population features with variant-specific features.

As an example, p.Pro347Ser, a variant with an observed 40% penetrance in the clinical cohort, would likely result in treatment intervention if clinically encountered by a clinician familiar with the variant through families seen in their clinic (Figure 6). However, from variant-specific features, our analysis generated a prior for p.Pro347Ser equivalent to observing only 1 in 10 heterozygous individuals diagnosed with LQT2. This new information could permit a more flexible approach to workup if no other information were known. A relatively high number of observations of p.Pro347Ser in the literature and gnomAD, which also suggest an LQT2 probability/penetrance of less than 5% for this variant (Figure 6), helps illustrate the calibration of our variant-informed priors. In this way, joint clinical phenotyping and tool utilization can be used in a mutually beneficial way for patients heterozygous for rare variants. We have developed an online searchable tool, the *KCNH2* Variant Browser (https://variantbrowser.org/KCNH2/), to allow rapid access to the estimated penetrance based on variant-specific features.

Limitations

One limitation is the bias inherent to each of the data sources used. We may be able to observe more carriers of these *KCNH2* variants as greater numbers of individuals are exome sequenced; however, for many variants, we may never observe more carriers and will be underpowered to estimate LQT2 probability by observation of heterozygotes alone. This fact is further motivation to establish a framework where experimental data is included quantitatively in the estimate of disease probability. The availability of functional data is also biased in that most variants which have these data available are from variants discovered in individuals presenting with a phenotype (Figure XIV in the Data Supplement); however, high-throughput variant functional characterization has the potential to overcome this bias.[42] Additionally, many factors influence the ultimate presentation of LQT2 in an individual, including genetic and environmental factors,[4,43,44] although we did not observe significant differences in predictive performance across nationality (Table III in the Data Supplement). Although the largest effect sizes for LQTS-associated variants come from rare variants, some of the variability in LQTS presentation can be explained by variability in common variants. Recently, 2 publications by Lahrouchi et al[45] and Turkowski et al[46] concluded polygenic risk scores accounted for ≈15% and <2% of the variability in LQTS susceptibility. Although in either case, the contribution is relatively small, it is possible polygenic risk is potentiated in the rare variant context and could therefore explain a greater portion of the variability in disease presentation. Lastly, although beyond the scope of the present study, we envision this method will enable improved prognostication of more severe presentations of LQT2 including arrhythmic events. Future work will address these exciting possibilities.

Conclusions

We have shown how variant-specific features can inform a prior probability of disease for rare variants even in the absence of clinically phenotyped heterozygotes. We have demonstrated this framework on the classical Mendelian disease-gene pair, LQT2, and *KCNH2*. We exploit in vitro functional studies, LQT2 probability density, and broad in silico predictors to calculate these priors. We then combine these estimates with patient data to form the posttest probability of disease for each variant. We have demonstrated that these in vitro and in silico variant features are equivalent to ≈10 clinically characterized heterozygotes when used to understand *KCNH2* variant-specific LQT2 disease probability. Presenting these data in this way allows us to encode both the probability of disease and the uncertainty in our estimates: we do not claim to have as much certainty as you would have if you phenotyped 100 heterozygotes; however, we do claim greater certainty than a single observation of a phenotyped heterozygote.

ARTICLE INFORMATION

Received October 26, 2020; accepted July 9, 2021.

Affiliations

Vanderbilt Center for Arrhythmia Research and Therapeutics (VanCART), Departments of Medicine & Pharmacology (K.K., Y.W., C.E., M.J.O., A.M.G., J.D.M., D.M.R.,

B.C.K., B.M.K.) and Division of Cardiovascular Medicine, Cardio-oncology Program (J.-E.S.), Vanderbilt University Medical Center, Nashville, TN. Department of Cardiovascular Medicine, Shiga University of Medical Science, Otsu, Japan (Y.W., S.O., M.H.). Laboratory of Cardiovascular Genetics, Istituto Auxologico Italiano IRCCS, Cusano Milanino, Italy (L.S., L.C., C.K., M.P., P.J.S.). CNMR Maladies Cardiaques Héréditaires Rares, AP-HP, Hôpital Bichat, Paris, France (I.D., A.L., F.E.). Department of Cardiovascular Medicine (T.A., N.M., S.O.) and 7Omics Research Center (N.M., T.I.), National Cerebral and Cardiovascular Center, Suita. Department of Cardiovascular Medicine, Graduate School of Medicine, Nippon Medical School, Tokyo, Japan (W.S.). Department of Cardiovascular, Neural & Metabolic Sciences, San Luca Hospital (L.C.) and Center for Cardiac Arrhythmias of Genetic Origin (L.C., C.S., F.D., S.C., P.J.S.), Istituto Auxologico Italiano IRCCS. Department of Medicine and Surgery, University Milano Bicocca, Milan (L.C.). Department of Molecular Medicine, Unit of Cardiology, University of Pavia (M.G.). Intensive Cardiac Care Unit and Lab of Experimental Cardiology for Cell and Molecular Therapy, Fondazione IRCCS Policlinico San Matteo, Pavia, Italy (M.G.). University de Paris (A.L., F.E.). Sorbonne Université, INSERM CIC-1901, AP-HP, Department of Pharmacology, Regional Pharmacovigilance Center, Pitié-Salpêtrière Hospital, Paris, France (J.-E.S.). Department of Biostatistics (Y.Z., J.D.M., D.M.R.) and Biomedical Informatics (J.D.M.), Vanderbilt University, Nashville, TN.

Sources of Funding

This work was supported by the National Institutes of Health grant number R00HL135442 (Dr Kroncke), the American Heart Association training grant 16FTF30130005 (Dr Mosley), and the Leducq Foundation for Cardiovascular Research grant 18CVD05 (Drs Egly, Crotti, Schwartz, Knollmann, and Kroncke), National Institutes of Health grant number R35HL144980 (Dr Knollmann), R01 HL149826 (Dr Roden), and K99 HG010904 (Dr Glazer), and Marie Skłodowska-Curie Individual Fellowship (H2020-MSCA-IF-2017; Grant Agreement No. 795209, Dr Sala).

Disclosures

None.

Supplemental Materials

Expanded Materials and Methods
Supplemental Tables I–III
Supplemental Figures I–XV
References [47–50]

REFERENCES

1. Tennessen JA, Bigham AW, O'Connor TD, Fu W, Kenny EE, Gravel S, McGee S, Do R, Liu X, Jun G, et al; Broad GO; Seattle GO; NHLBI Exome Sequencing Project. Evolution and functional impact of rare coding variation from deep sequencing of human exomes. *Science*. 2012;337:64–69. doi: 10.1126/science.1219240
2. Dewey FE, Murray MF, Overton JD, Habegger L, Leader JB, Fetterolf SN, O'Dushlaine C, Van Hout CV, Staples J, Gonzaga-Jauregui C, et al. Distribution and clinical impact of functional variants in 50,726 whole-exome sequences from the DiscovEHR Study. *Science*. 2016;354:aaf6814. doi: 10.1126/science.aaf6814
3. Lacaze P, Sebra R, Riaz M, Tiller J, Revote J, Phung J, Parker EJ, Orchard SG, Lockery JE, Wolfe R, et al. Medically actionable pathogenic variants in a population of 13,131 healthy elderly individuals. *Genet Med*. 2020;22:1883–1886. doi: 10.1038/s41436-020-0881-7
4. Schwartz PJ, Crotti L, George AL Jr. Modifier genes for sudden cardiac death. *Eur Heart J*. 2018;39:3925–3931. doi: 10.1093/eurheartj/ehy502
5. Richards S, Aziz N, Bale S, Bick D, Das S, Gastier-Foster J, Grody WW, Hegde M, Lyon E, Spector E, et al; ACMG Laboratory Quality Assurance Committee. Standards and guidelines for the interpretation of sequence variants: a joint consensus recommendation of the American College of Medical Genetics and Genomics and the Association for Molecular Pathology. *Genet Med*. 2015;17:405–424. doi: 10.1038/gim.2015.30
6. Tavtigian SV, Greenblatt MS, Harrison SM, Nussbaum RL, Prabhu SA, Boucher KM, Biesecker LG; ClinGen Sequence Variant Interpretation Working Group (ClinGen SVI). Modeling the ACMG/AMP variant classification guidelines as a Bayesian classification framework. *Genet Med*. 2018;20:1054–1060. doi: 10.1038/gim.2017.210
7. McClellan J, King MC. Genetic heterogeneity in human disease. *Cell*. 2010;141:210–217. doi: 10.1016/j.cell.2010.03.032
8. Badano JL, Katsanis N. Beyond Mendel: an evolving view of human genetic disease transmission. *Nat Rev Genet*. 2002;3:779–789. doi: 10.1038/nrg910
9. Walsh R, Thomson KL, Ware JS, Funke BH, Woodley J, McGuire KJ, Mazzarotto F, Blair E, Seller A, Taylor JC, et al. Reassessment of Mendelian gene pathogenicity using 7,855 cardiomyopathy cases and 60,706 reference samples. *Genet Med*. 2017;19:192–203. doi: 10.1038/gim.2016.90
10. Hosseini SM, Kim R, Udupa S, Costain G, Jobling R, Liston E, Jamal SM, Szybowska M, Morel CF, Bowdin S, et al; National Institutes of Health Clinical Genome Resource Consortium. Reappraisal of reported genes for sudden arrhythmic death: evidence-based evaluation of gene validity for brugada syndrome. *Circulation*. 2018;138:1195–1205. doi: 10.1161/CIRCULATIONAHA.118.035070
11. Kroncke BM, Smith DK, Zuo Y, Glazer AM, Roden DM, Blume JD. A Bayesian method to estimate variant-induced disease penetrance. *PLoS Genet*. 2020;16:e1008862. doi: 10.1371/journal.pgen.1008862
12. Perrin MJ, Subbiah RN, Vandenberg JI, Hill AP. Human ether-a-go-go related gene (hERG) K+ channels: function and dysfunction. *Prog Biophys Mol Biol*. 2008;98:137–148. doi: 10.1016/j.pbiomolbio.2008.10.006
13. Bohnen MS, Peng G, Robey SH, Terrenoire C, Iyer V, Sampson KJ, Kass RS. Molecular pathophysiology of congenital long QT syndrome. *Physiol Rev*. 2017;97:89–134. doi: 10.1152/physrev.00008.2016
14. Kapa S, Tester DJ, Salisbury BA, Harris-Kerr C, Pungliya MS, Alders M, Wilde AA, Ackerman MJ. Genetic testing for long-QT syndrome: distinguishing pathogenic mutations from benign variants. *Circulation*. 2009;120:1752–1760. doi: 10.1161/CIRCULATIONAHA.109.863076
15. Walsh R, Lahrouchi N, Tadros R, Kyndt F, Glinge C, Postema PG, Amin AS, Nannenberg EA, Ware JS, Whiffin N, et al; Nantes Referral Center for inherited cardiac arrhythmia. Enhancing rare variant interpretation in inherited arrhythmias through quantitative analysis of consortium disease cohorts and population controls. *Genet Med*. 2021;23:47–58. doi: 10.1038/s41436-020-00946-5
16. Ioannidis NM, Rothstein JH, Pejaver V, Middha S, McDonnell SK, Baheti S, Musolf A, Li Q, Holzinger E, Karyadi D, et al. REVEL: an ensemble method for predicting the pathogenicity of rare missense variants. *Am J Hum Genet*. 2016;99:877–885. doi: 10.1016/j.ajhg.2016.08.016
17. Crotti L, Lundquist AL, Insolia R, Pedrazzini M, Ferrandi C, De Ferrari GM, Vicentini A, Yang P, Roden DM, George AL Jr, et al. KCNH2-K897T is a genetic modifier of latent congenital long-QT syndrome. *Circulation*. 2005;112:1251–1258. doi: 10.1161/CIRCULATIONAHA.105.549071
18. Lek M, Karczewski KJ, Minikel EV, Samocha KE, Banks E, Fennell T, O'Donnell-Luria AH, Ware JS, Hill AJ, Cummings BB, et al; Exome Aggregation Consortium. Analysis of protein-coding genetic variation in 60,706 humans. *Nature*. 2016;536:285–291. doi: 10.1038/nature19057
19. Fodstad H, Bendahhou S, Rougier JS, Laitinen-Forsblom PJ, Barhanin J, Abriel H, Schild L, Kontula K, Swan H. Molecular characterization of two founder mutations causing long QT syndrome and identification of compound heterozygous patients. *Ann Med*. 2006;38:294–304. doi: 10.1080/07853890600756065
20. Lahti AL, Kujala VJ, Chapman H, Koivisto AP, Pekkanen-Mattila M, Kerkelä E, Hyttinen J, Kontula K, Swan H, Conklin BR, et al. Model for long QT syndrome type 2 using human iPS cells demonstrates arrhythmogenic characteristics in cell culture. *Dis Model Mech*. 2012;5:220–230. doi: 10.1242/dmm.008409
21. Fodstad H, Swan H, Laitinen P, Piippo K, Paavonen K, Viitasalo M, Toivonen L, Kontula K. Four potassium channel mutations account for 73% of the genetic spectrum underlying long-QT syndrome (LQTS) and provide evidence for a strong founder effect in Finland. *Ann Med*. 2004;36(suppl 1):53–63. doi: 10.1080/17431380410032689
22. Cui J, Kagan A, Qin D, Mathew J, Melman YF, McDonald TV. Analysis of the cyclic nucleotide binding domain of the HERG potassium channel and interactions with KCNE2. *J Biol Chem*. 2001;276:17244–17251. doi: 10.1074/jbc.M010904200
23. Benhorin J, Moss AJ, Bak M, Zareba W, Kaufman ES, Kerem B, Towbin JA, Priori S, Kass RS, Attali B, et al. Variable expression of long QT syndrome among gene carriers from families with five different HERG mutations. *Ann Noninvasive Electrocardiol*. 2002;7:40–46. doi: 10.1111/j.1542-474x.2001.tb00137.x
24. Satler CA, Walsh EP, Vesely MR, Plummer MH, Ginsburg GS, Jacob HJ. Novel missense mutation in the cyclic nucleotide-binding domain of HERG causes long QT syndrome. *Am J Med Genet*. 1996;65:27–35. doi: 10.1002/(SICI)1096-8628(19961002)65:1<27::AID-AJMG4>3.0.CO;2-V
25. Sanguinetti MC, Curran ME, Spector PS, Keating MT. Spectrum of HERG K+-channel dysfunction in an inherited cardiac arrhythmia. *Proc Natl Acad Sci U S A*. 1996;93:2208–2212. doi: 10.1073/pnas.93.5.2208
26. Anderson CL, Delisle BP, Anson BD, Kilby JA, Will ML, Tester DJ, Gong Q, Zhou Z, Ackerman MJ, January CT. Most LQT2 mutations reduce Kv11.1

(hERG) current by a class 2 (trafficking-deficient) mechanism. *Circulation*. 2006;113:365–373. doi: 10.1161/CIRCULATIONAHA.105.570200
27. Mehta A, Sequiera GL, Ramachandra CJ, Sudibyo Y, Chung Y, Sheng J, Wong KY, Tan TH, Wong P, Liew R, et al. Re-trafficking of hERG reverses long QT syndrome 2 phenotype in human iPS-derived cardiomyocytes. *Cardiovasc Res*. 2014;102:497–506. doi: 10.1093/cvr/cvu060
28. Li G, Shi R, Wu J, Han W, Zhang A, Cheng G, Xue X, Sun C. Association of the hERG mutation with long-QT syndrome type 2, syncope and epilepsy. *Mol Med Rep*. 2016;13:2467–2475. doi: 10.3892/mmr.2016.4859
29. Goldenberg I, Horr S, Moss AJ, Lopes CM, Barsheshet A, McNitt S, Zareba W, Andrews ML, Robinson JL, Locati EH, et al. Risk for life-threatening cardiac events in patients with genotype-confirmed long-QT syndrome and normal-range corrected QT intervals. *J Am Coll Cardiol*. 2011;57:51–59. doi: 10.1016/j.jacc.2010.07.038
30. Shimizu W, Moss AJ, Wilde AA, Towbin JA, Ackerman MJ, January CT, Tester DJ, Zareba W, Robinson JL, Qi M, et al. Genotype-phenotype aspects of type 2 long QT syndrome. *J Am Coll Cardiol*. 2009;54:2052–2062. doi: 10.1016/j.jacc.2009.08.028
31. Wang W, MacKinnon R. Cryo-EM structure of the open human ether-à-go-go-related K+ channel hERG. *Cell*. 2017;169:422–430.e10. doi: 10.1016/j.cell.2017.03.048
32. Wright CF, West B, Tuke M, Jones SE, Patel K, Laver TW, Beaumont RN, Tyrrell J, Wood AR, Frayling TM, et al. Assessing the pathogenicity, penetrance, and expressivity of putative disease-causing variants in a population setting. *Am J Hum Genet*. 2019;104:275–286. doi: 10.1016/j.ajhg.2018.12.015
33. Minikel EV, Zerr I, Collins SJ, Ponto C, Boyd A, Klug G, Karch A, Kenny J, Collinge J, Takada LT, et al. Ascertainment bias causes false signal of anticipation in genetic prion disease. *Am J Hum Genet*. 2014;95:371–382. doi: 10.1016/j.ajhg.2014.09.003
34. Marjamaa A, Salomaa V, Newton-Cheh C, Porthan K, Reunanen A, Karanko H, Jula A, Lahermo P, Väänänen H, Toivonen L, et al. High prevalence of four long QT syndrome founder mutations in the Finnish population. *Ann Med*. 2009;41:234–240. doi: 10.1080/07853890802668530
35. Christiansen M, Hedley PL, Theilade J, Stoevring B, Leren TP, Eschen O, Sørensen KM, Tybjærg-Hansen A, Ousager LB, Pedersen LN, et al. Mutations in Danish patients with long QT syndrome and the identification of a large founder family with p.F29L in KCNH2. *BMC Med Genet*. 2014;15:31. doi: 10.1186/1471-2350-15-31
36. Tester DJ, Will ML, Haglund CM, Ackerman MJ. Compendium of cardiac channel mutations in 541 consecutive unrelated patients referred for long QT syndrome genetic testing. *Heart Rhythm*. 2005;2:507–517. doi: 10.1016/j.hrthm.2005.01.020
37. Mechakra A, Vincent Y, Chevalier P, Millat G, Ficker E, Jastrzebski M, Poulin H, Pouliot V, Chahine M, Christé G. The variant hERG/R148W associated with LQTS is a mutation that reduces current density on co-expression with the WT. *Gene*. 2014;536:348–356. doi: 10.1016/j.gene.2013.11.072
38. Saenen JB, Paulussen AD, Jongbloed RJ, Marcelis CL, Gilissen RA, Aerssens J, Snyders DJ, Raes AL. A single hERG mutation underlying a spectrum of acquired and congenital long QT syndrome phenotypes. *J Mol Cell Cardiol*. 2007;43:63–72. doi: 10.1016/j.yjmcc.2007.04.012
39. Millat G, Chevalier P, Restier-Miron L, Da Costa A, Bouvagnet P, Kugener B, Fayol L, Gonzàlez Armengod C, Oddou B, Chanavat V, et al. Spectrum of pathogenic mutations and associated polymorphisms in a cohort of 44 unrelated patients with long QT syndrome. *Clin Genet*. 2006;70:214–227. doi: 10.1111/j.1399-0004.2006.00671.x
40. Lane CM, Giudicessi JR, Ye D, Tester DJ, Rohatgi RK, Bos JM, Ackerman MJ. Long QT syndrome type 5-Lite: Defining the clinical phenotype associated with the potentially proarrhythmic p.Asp85Asn-KCNE1 common genetic variant. *Heart Rhythm*. 2018;15:1223–1230. doi: 10.1016/j.hrthm.2018.03.038
41. Giudicessi JR, Roden DM, Wilde AAM, Ackerman MJ. Classification and reporting of potentially proarrhythmic common genetic variation in long QT syndrome genetic testing. *Circulation*. 2018;137:619–630. doi: 10.1161/CIRCULATIONAHA.117.030142
42. Kozek KA, Glazer AM, Ng CA, Blackwell D, Egly CL, Vanags LR, Blair M, Mitchell D, Matreyek KA, Fowler DM, et al. High-throughput discovery of trafficking-deficient variants in the cardiac potassium channel KV11.1. *Heart Rhythm*. 2020;17:2180–2189. doi: 10.1016/j.hrthm.2020.05.041
43. Cooper DN, Krawczak M, Polychronakos C, Tyler-Smith C, Kehrer-Sawatzki H. Where genotype is not predictive of phenotype: towards an understanding of the molecular basis of reduced penetrance in human inherited disease. *Hum Genet*. 2013;132:1077–1130. doi: 10.1007/s00439-013-1331-2
44. Castel SE, Cervera A, Mohammadi P, Aguet F, Reverter F, Wolman A, Guigo R, Iossifov I, Vasileva A, Lappalainen T. Modified penetrance of coding variants by cis-regulatory variation contributes to disease risk. *Nat Genet*. 2018;50:1327–1334. doi: 10.1038/s41588-018-0192-y
45. Lahrouchi N, Tadros R, Crotti L, Mizusawa Y, Postema PG, Beekman L, Walsh R, Hasegawa K, Barc J, Ernsting M, et al. Transethnic genome-wide association study provides insights in the genetic architecture and heritability of long QT syndrome. *Circulation*. 2020;142:324–338. doi: 10.1161/CIRCULATIONAHA.120.045956
46. Turkowski KL, Dotzler SM, Tester DJ, Giudicessi JR, Bos JM, Speziale AD, Vollenweider JM, Ackerman MJ. Corrected QT interval-polygenic risk score and its contribution to type 1, type 2, and type 3 long-QT syndrome in probands and genotype-positive family members. *Circ Genom Precis Med*. 2020;13:e002922. doi: 10.1161/CIRCGEN.120.002922
47. Schwartz PJ, Stramba-Badiale M, Crotti L, Pedrazzini M, Besana A, Bosi G, Gabbarini F, Goulene K, Insolia R, Mannarino S, et al. Prevalence of the congenital long-QT syndrome. *Circulation*. 2009;120:1761–1767. doi: 10.1161/CIRCULATIONAHA.109.863209
48. Priori SG, Wilde AA, Horie M, Cho Y, Behr ER, Berul C, Blom N, Brugada J, Chiang CE, Huikuri H, et al. HRS/EHRA/APHRS expert consensus statement on the diagnosis and management of patients with inherited primary arrhythmia syndromes: document endorsed by HRS, EHRA, and APHRS in May 2013 and by ACCF, AHA, PACES, and AEPC in June 2013. *Heart Rhythm*. 2013;10:1932–1963. doi: 10.1016/j.hrthm.2013.05.014
49. Schwartz PJ, Moss AJ, Vincent GM, Crampton RS. Diagnostic criteria for the long QT syndrome. An update. *Circulation*. 1993;88:782–784. doi: 10.1161/01.cir.88.2.782
50. Kroncke BM, Mendenhall J, Smith DK, Sanders CR, Capra JA, George AL, Blume JD, Meiler J, Roden DM. Protein structure aids predicting functional perturbation of missense variants in SCN5A and KCNQ1. *Comput Struct Biotechnol J*. 2019;17:206–214. doi: 10.1016/j.csbj.2019.01.008